Journal of Alloys and Compounds 253–254 (1997) 492–495

Journal of
ALLOYS
AND COMPOUNDS

Microstructural characterisation of surface layers of ZrM_2 powders (Laves phases) obtained by various corrosion treatments

M. Backhaus-Ricoult[a,*], J.L. Vignes[a], G. Lorang[a], B. Knosp[b]

[a]*Centre d'Etudes de Chimie Métallurgique, CNRS, 15 Rue G. Urbain, 94407 Vitry, France*
[b]*Alcatel Alsthom Recherche, 91460 Marcoussis, France*

Abstract

C14 and C15 Laves phase alloys containing Zr, Ni, Mn, V and Ti as major alloy constituents are exposed to air and subsequently treated in various aqueous solutions, such as diluted hydrofluoric acid and concentrated alkaline solution. Corrosion products at the surface of the alloy powders are analyzed by transmission electron microscopy (TEM) and Auger spectroscopy to identify their chemical composition and crystal structure.

Keywords: Laves phase; Corrosion; Microstructure

1. Introduction

Zirconium-based Laves phase alloys have a high potential for application as electrode materials in reversible metal hydride batteries. However, surface oxide layers prevent hydrogen absorption, and an electrochemical activation of the electrodes is necessary to reach satisfactory battery capacities. The efficiency of the activation procedure depends on the corrosion products forming in air at the surface of the alloy and on the type of activation treatment chosen.

2. Materials and corrosion treatments

In the present paper, we investigate two Laves phase alloys, L72, a C15-type cubic alloy with lattice parameter 0.7068 nm, and L12, a C14-type hexagonal alloy with lattice parameters $a=0.4999$ nm and $b=0.8154$ nm. The compositions are as follows:

	Zr	Ti	Ni	Mn	Al	V	Cr	Co
L12	0.8	0.2	0.8	0.8	0.05	0.2		0.15
L72	1.0	–	1.2	0.6		0.2	0.1	

Homogeneous alloy ingots are obtained by melting and casting in an induction furnace under argon atmosphere and further annealing at 1050 °C for 150 h, under vacuum. Powders for TEM investigations are prepared from the ingots by repeated adsorption and desorption of hydrogen gas, followed by mechanical grinding under an argon atmosphere. The alloys are exposed to air at room temperature and afterwards treated in different aqueous solutions, such as diluted hydrofluoric acid (0.25 M) at room temperature and a concentrated alkaline solution (8.7 M) at 70 °C. Chemical analysis of the solutions after the treatments shows that vanadium, zirconium and manganese are the most soluble elements.

3. Analysis of the corrosion scales

The surface scales of the alloy ingots and powders are examined after oxidation in air and after the different treatments, by Auger spectroscopy (AES) depth profiling and by traditional and analytical transmission electron microscopy, respectively. AES surface analysis provides good depth resolution (despite poor lateral resolution) and yields information on the oxidation state of the elements in presence. TEM brings the complementary high spatial resolution (as good as a few square nm). In addition, this latter technique allows us to obtain information on the scale morphology (by imaging techniques), as well as on the chemical (by EDX analysis) and crystallographic (by electron diffraction) nature of the phases.

For TEM investigations, powders of approximately

---

[*] Corresponding author.

0925-8388/97/$17.00 © 1997 Elsevier Science S.A. All rights reserved
PII S0925-8388(96)03033-2

1 μm grain size are deposited under an argon atmosphere on a copper grit and immediately introduced into the microscope chamber, in order to avoid oxidation. A JEOL 200FX microscope equipped with a Link EDX detector for light element analysis is used for the study. AES derivative spectra are acquired at 2.5 keV primary electron beam energy with a CMA analyzer (Riber-OPC 105) between sputtering sequences performed with 3.0 keV Kr ions (etching rate 0.15–0.5 nm mn^{-1}). Due to their low signal-to-noise ratio, no significant signal evolution of titanium, vanadium and cobalt intensities can be reported.

4. Experimental results

4.1. Oxidation in air

TEM observations made on the C14 and C15 Laves phase powders indicate that exposure to air produces more or less continuous nanocrystalline mixed oxide layers. Their grain size depends on the type of alloy: 20–50 nm for L72 and 2–10 nm for L12. The oxides are identified as a zirconium-rich mixed oxide having the crystal structure of baddeleite and containing vanadium, titanium, (chromium) and nickel in solid solution, and as a phase enriched in nickel oxide, with fcc (NiO) structure (Fig. 1a).

AES depth profiles (Fig. 1b) on polished ingots show superficial oxidized films (1–2 nm on L12 and 3–4 nm on L72), which are enriched in nickel (L72) and manganese (L12) in their outer part and in zirconium in more depth (extending up to the oxide–alloy interface).

4.2. Treatment in diluted HF

Treatment of the oxidized powders in diluted HF yields dissolution of the oxide scale and preferential leaching of some of the alloy constituents. TEM observations reveal rare residues of the oxide layers, most of the surface being free of oxide particles. However, as a result of this treatment, the alloy undergoes partial or complete amorphisation, and frequently nanocrystalline or amorphous surface scales are observed on the powder particles (Fig. 2a). The alloy close to the particle surfaces is depleted in zirconium and aluminum. The corrosion scale consists of a mixture of metallic nickel and manganese, which contains

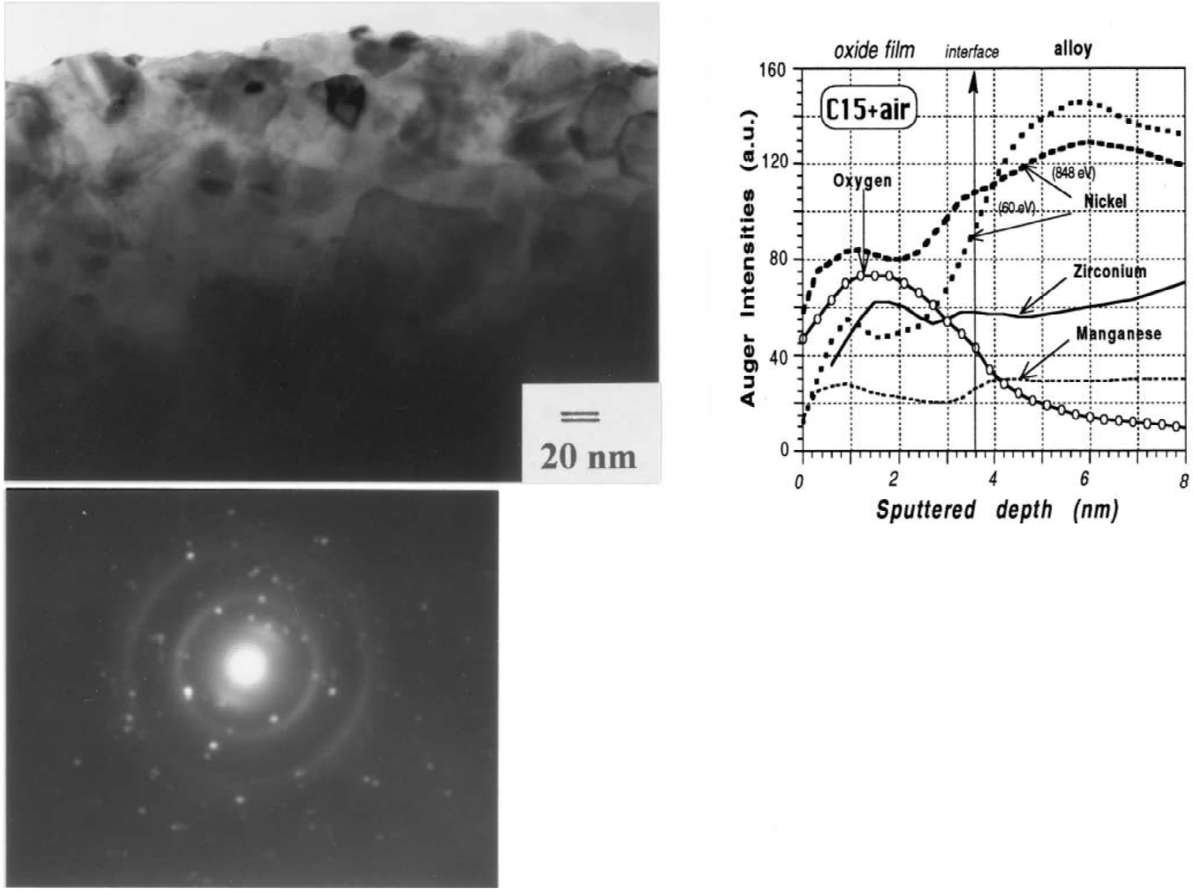

Fig. 1. L72 oxidized in air: (a) TEM bright-field image of the corrosion scale together with corresponding diffraction pattern, and (b) AES depth profiles.

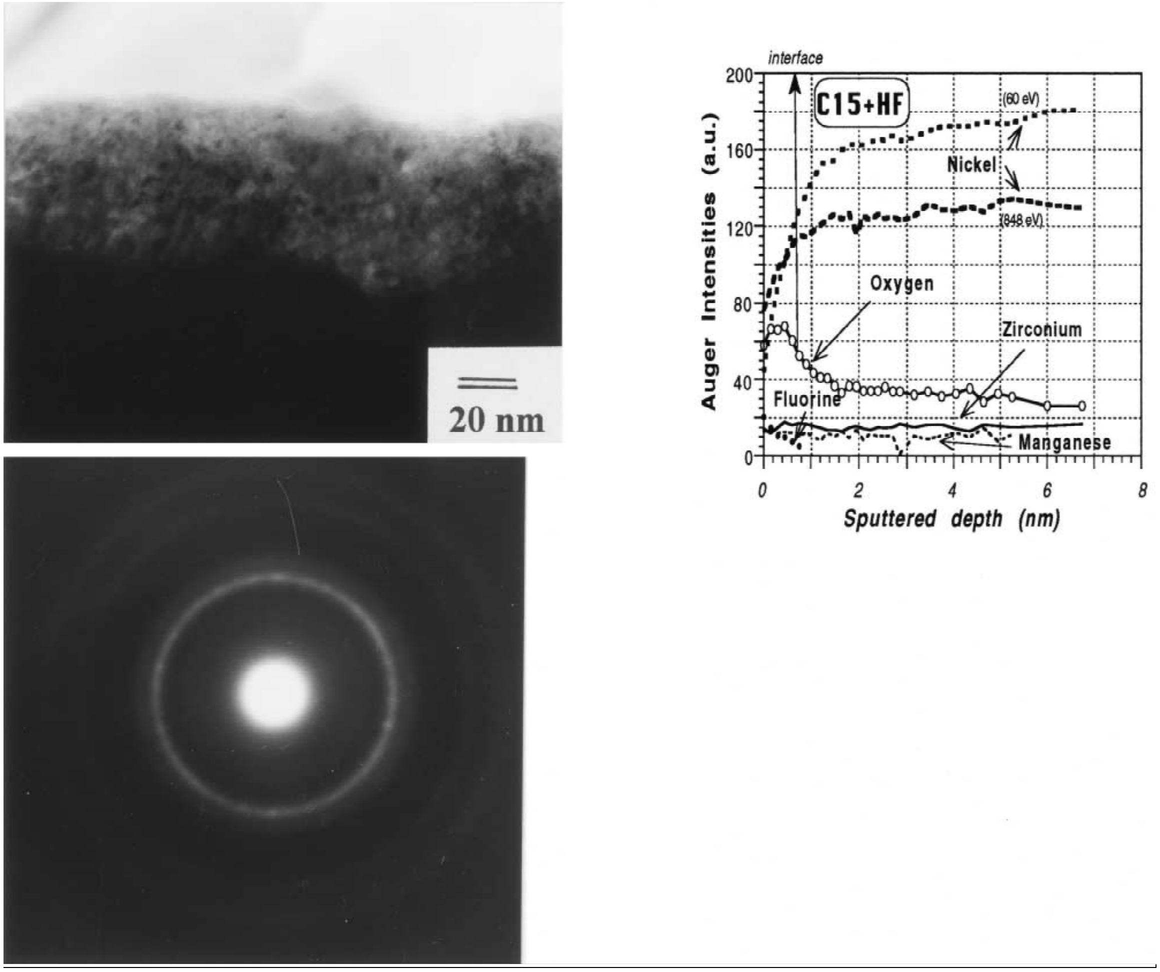

Fig. 2. L72 oxidized in air and etched in HF: (a) TEM bright-field image of the corrosion scale with corresponding diffraction pattern, and (b) AES depth profiles.

small amounts of titanium, vanadium and cobalt, and adopts the Ni fcc crystal structure. Nickel oxide and mixed spinel of nickel and manganese are detected in small amounts in the surface scale. In nickel-rich L72 alloy, the surface scale contains much less manganese and contains up to 90% nickel. Only negligible quantities of oxygen and fluorine are detected in the scale.

AES depth profiles globally support the TEM results. The surface alloy is found to be almost free of oxides for L72 (1 nm thickness), but notable contents of carbon (and fluorine for L12) are present. Important zirconium and manganese depletion in the surface-close alloy and enrichment in nickel over thicknesses larger than 8 nm are detected (Fig. 2b). ICP analysis of solutions confirms the preferential dissolution of zirconium and manganese, which seems to prevent the material from formation of stable Zr–Mn oxide layers in atmosphere. HF treatment is less efficient for the L12 alloy considering the remaining oxygen content and the diffuse interface.

4.3. Treatment in concentrated KOH

Powder surfaces show an important increase in roughness after treatment in KOH. The nanocrystalline zirconia scale due to oxidation in air is no longer present. Instead, layered structures, about 20 nm thick and identified as textured (Ni,Mn)O mixed oxide, cover the surface. Single crystalline needles of manganite, up to a few nm in length, stick out of the particle surfaces. They are surrounded by nanocrystalline or sub-amorphous mixtures of baddeleite (ZrO_2 enriched in Ti, V and Al), substituted manganosite ((Mn,Ni)O) and manganite (MnO(OH)). Inside the corrosion layer, distinct metal nanoparticles are found: (Ni,Co) in the case of L12 and nickel–manganese-rich alloys (containing small amounts of Ti, V, Cr and Zr) in the case of L72. A typical scale is shown in Fig. 3a.

As for films formed in air, depth profiles of corrosion films formed in KOH solution (2–3 nm thickness for L72 and 9–12 nm for L12) show an outer layer enriched in

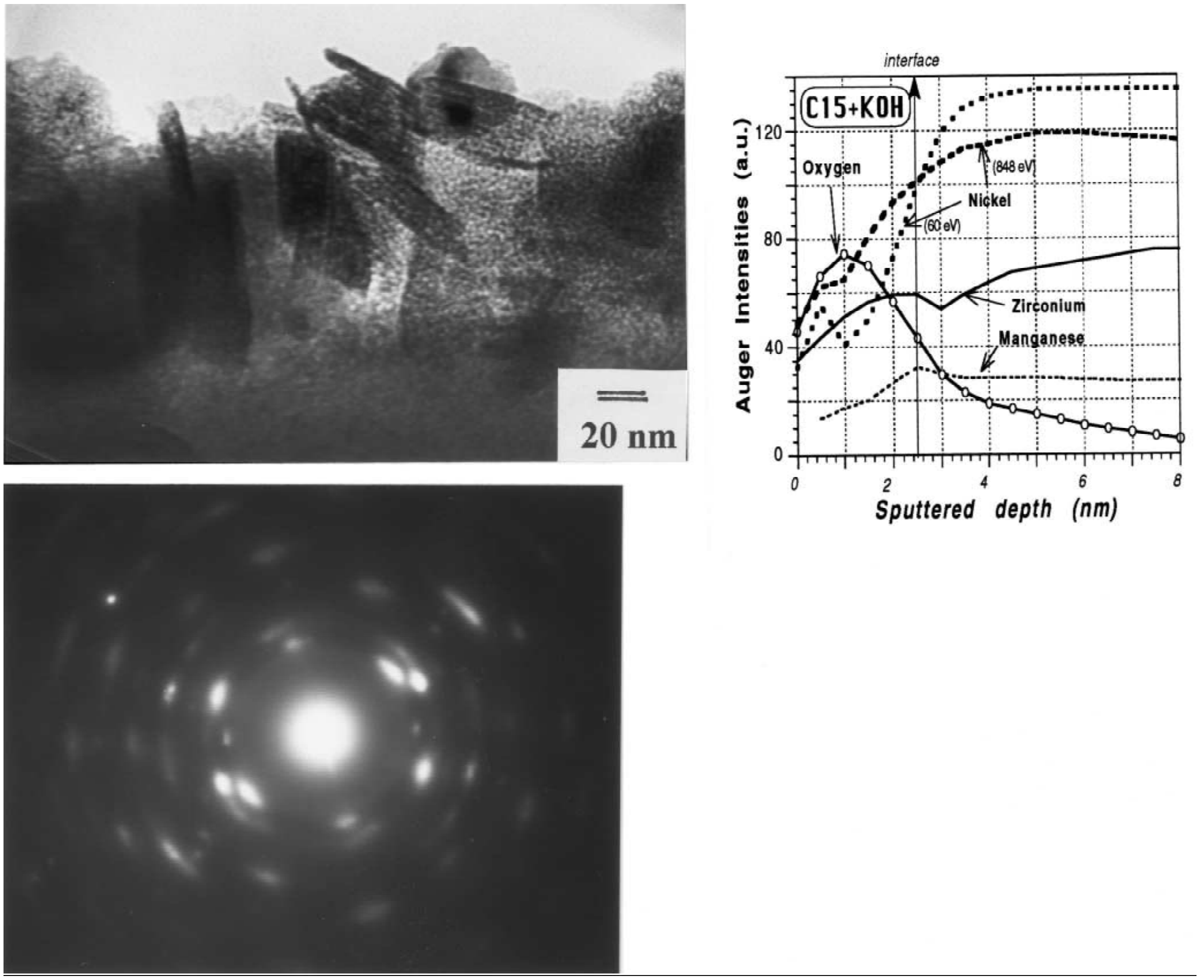

Fig. 3. L72 oxidised in air and etched in concentrated KOH: (a) TEM bright-field image of a tilted corrosion scale with corresponding diffraction pattern, and (b) AES depth profiles.

oxidized nickel (and manganese for L12) which covers a zirconium-rich layer extending up to the oxide–alloy interface (Fig. 3b).

Acknowledgments

The authors wish to gratefully acknowledge the financial support from SAFT/Alcatel Alsthom Recherche, which made this work possible.